

A TECHNIQUE FOR THE REDUCTION AND ANALYSIS OF  
OCEAN SPECTRAL DATA

By

Peter G. White  
TRW Systems Group  
Redondo Beach, Calif.

INTRODUCTION

One of the most difficult problems associated with the interpretation of remote spectral measurements of the ocean is the separation of atmospheric effects from the signal which originates in the water. The total signal received by a high altitude aircraft or spacecraft contains information originating in both the water itself and the atmosphere, with the latter predominating.

Because the user of these data is interested in the difference between the spectral radiance of various bodies of water, he finds it necessary to measure small percentage differences in radiance, even though the basic differences in the signal from the water bodies may be substantial. This is illustrated by the following:

$$S_T = S_A + S_W$$

where  $S_T$ ,  $S_A$  and  $S_W$  are the signal received at the sensor, and the individual components from the atmosphere and the water, respectively.  $S_A$  is large compared to  $S_W$ ; typically larger by a factor of 10 in the case of a spacecraft measurement. Thus an uncertainty of 1% in  $S_T$  can result in an uncertainty of 10% in deriving  $S_W$ . This imposes severe accuracy and sensitivity requirements on the measurement of  $S_T$  and on the calibration of the instrument which makes these measurements.

The following paragraphs describe some initial investigations of a method of reducing and analyzing raw ocean spectral data which avoids most of the problems associated with atmospheric effects, and which requires the application of little if any calibration information to the data.

ANALYSIS OF RAW SPECTRAL DATA

Figure 1 shows unreduced spectral curves of two bodies of water as sensed from 1,000 ft. altitude. The data are in arbitrary units and are described by the following:

$$S_{\lambda} = [IR(\rho_W^{\tau} + \rho_A)]_{\lambda} G$$

where

$S_{\lambda}$  is the ordinate of Figure 1

$I$  is the solar spectral irradiance at the ocean surface

$R$  is the spectral response of the measuring instrument

$\rho_W$  is the spectral reflectivity of the ocean

$\rho_A$  is the effective spectral reflectivity of the atmosphere

$\tau$  is the spectral transmission of the atmosphere from the surface to the measurement altitude

$G$  is an instrument conversion factor.

The data were taken with a rapid scanning spectrometer and the curves of Figure 1 represent the analog output of the instrument. The spectrometer has a spectral resolution of 10 nm. Figure 2 shows spectral curves of the same two water bodies as measured from 25,000 ft. altitude.

A comparison of the two figures shows that differences between the two water bodies are much more apparent at the lower altitude (Figure 1). At higher altitude (Figure 2) the additive light backscattered by the atmosphere significantly reduces the percentage differences between the curves. In spite of this, features due to differences between the two types of water may be distinguished on Figure 2 as well as Figure 1.

In order to enhance these differences and at the same time reject the information contained in the general shape of the curve (spectral response of the instrument, spectral irradiance of the sun, and atmospheric radiance) the second derivative of each of the four curves has been calculated and plotted in Figures 3 and 4.

Note that certain features of the derivative curves appear to be relatively independent of altitude.

In order to identify spectral regions which are most sensitive to changes in water color and least sensitive to atmospheric effects, the following technique has been used to isolate the relative effects of each.

Figure 5 is a plot of the difference in second derivatives ( $S''_B - S''_A$ ) of the two types of water (identified as A and B for convenience). <sup>B</sup>Note that the curves are strikingly similar regardless of altitude. Similarly Figure 6 is a plot of the difference of the second derivatives of the two altitudes ( $S''_{1000} - S''_{25,000}$ ). The similarity between the curves here is even more marked, indicating that we have successfully isolated the effects on the second derivative of water color (Figure 5) and atmosphere (Figure 6).

In order to determine the spectral regions in which water color effects on the second derivative predominate over atmospheric effects, Figure 7 has been prepared showing the subtractive difference between the curves of

Figures 5 and 6. Those portions of the curve below zero (atmospheric effect greater than water color effect) have not been plotted. Regions of maximum difference are centered at 486, 570, 604, and 655 nanometers. It is suggested that second derivatives of raw spectral curves be evaluated at these wavelengths in order to minimize atmospheric effects and give maximum information about the water type. However it is probable that other types of water will yield additional wavelengths well suited for discrimination.

### PRACTICAL CONSIDERATIONS IN USING THE TECHNIQUE

As stated earlier, the spectral resolution of the raw data is 10 nm. In order to determine the effect of spectral resolution on the technique, the raw data was degraded to 30 nm resolution by passing a "moving window" numerical filter of 30 nm width over the data and then again calculating the second derivatives. Figure 8 is an example of the 30 nm raw data compared to the 10 nm data. There is a general smoothing of the curve at 30 nm.

Figure 9 shows the second derivatives of the Figure 8 (30 nm resolution) data. A measure of the information lost by degrading the resolution from 10 to 30 nm is the difference in amplitude of the curve from 570 to 604 nm. On this basis the information lost (amplitude reduction) is 21%.

In calculating the second derivative, another spectral filter is used in the calculation as follows:

$$S''_{\lambda+\beta/2} = (S_{\lambda} - S_{\lambda+\beta}) - (S_{\lambda+\Delta\lambda} - S_{\lambda+\Delta\lambda+\beta})$$

where  $\beta$  is the spectral bandpass of the filter and  $\Delta\lambda$  is wavelength interval between calculations (5 nm in the examples given). All of the previous examples have used a  $\beta$  of 30 nm. This appears to be approximately optimum to maximize differences between the curves, but for comparison, Figure 10 shows the effect of reducing  $\beta$  to 10 nm. Considerably more structure is apparent in the curve, but it is not clear at this time how much is due to Fraunhofer lines, atmospheric absorptions and noise as opposed to water color information.

The effect of increasing  $\Delta\lambda$  to 15 nm from 5 nm (decreasing sampling rate by a factor of 3) is shown in the second derivative plots of Figure 11. The advantage of maintaining  $\Delta\lambda$  at 5 nm is obvious.

Another important factor in using this method is the need for data which has been acquired in a "moving window" type of spectral scan as opposed to individual detectors located in each of the spectral bands. A moving window scan is one in which an aperture, whose width defines the spectral resolution is moved at a constant velocity over the spectrum to be analyzed. If this is not done (i.e., if separate detectors are located in different regions of the spectrum) then it is necessary to mathematically fit a curve from point to point through the spectrum to reduce  $\Delta\lambda$ . The characteristics of the equation used to fit the curve will then have a strong undesirable influence on the second derivative.

### MEASUREMENT SENSITIVITY

The potential sensitivity of the second derivative technique can be illustrated by comparing data from the two bodies of water shown in Figure 2 as measured from 25,000 ft. altitude. Although the actual content of plankton in each type of water is not known exactly, surface truth measurements established that the type A water contained approximately ten times the plankton of type B. If we consider the excursion of the second derivative from 570 to 604 nanometers to be an indicator of plankton content, then the value of this indicator increased by 3.7 times from type B to type A. This suggests a non-linear relationship between the indicator and the plankton content, and/or a positive value of the indicator when the plankton count is zero. However, the maximum apparent noise or scatter on the derivative curves is less than one part in 50 of the range of the indicator which implies that the water may be categorized into some 25 levels between the limits shown. It is not expected that the clarity or haze content of the atmosphere will have an appreciable effect on these accuracies for sun zenith angles of less than  $40^\circ$  and viewing angles less than  $10^\circ$  off the nadir.<sup>1</sup>

### CONCLUSIONS

1. The analysis technique described is capable of distinguishing fairly subtle differences in water color from data which has been measured through an atmosphere with at least half the optical density of the earth's total atmosphere.
2. The technique does not require the application of calibrations to the raw data, other than a simple correction for solar elevation angle.
3. Data obtained at 30 nm spectral resolution has about 20% less information content than data with 10 nm resolution.
4. Data should be obtained with a single "moving window" type spectral scan, with individual digitized samples about 5 nm apart.

---

<sup>1</sup> R. S. Fraser and R. C. Ramsey, "Nadir Spectral Radiance of the Sunlit Earth as Viewed from above the Atmosphere," TRW Internal Publication.

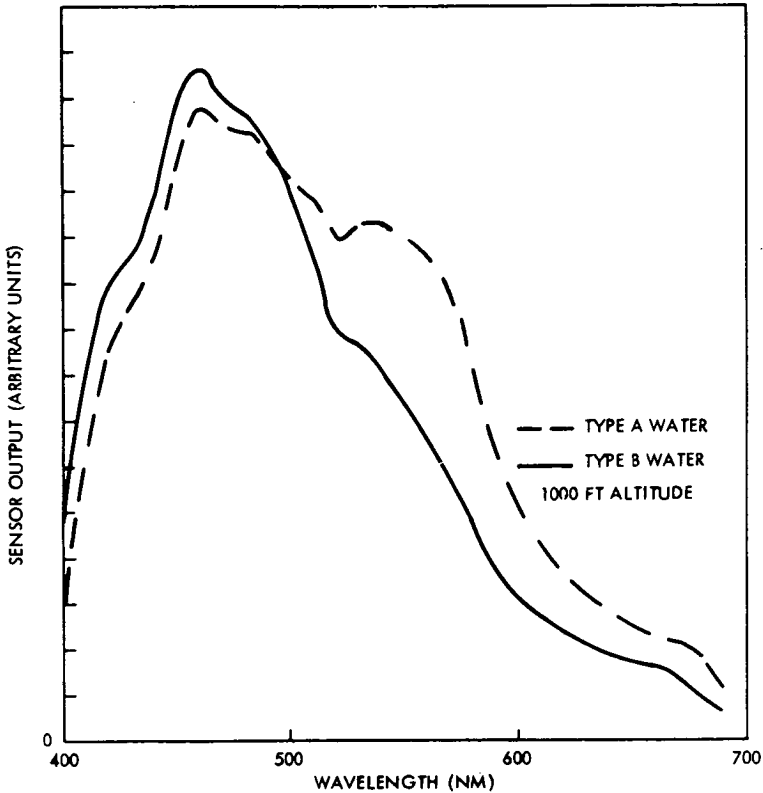


FIGURE 1. UNREDUCED SENSOR OUTPUT SIGNAL - 1000 FT ALTITUDE

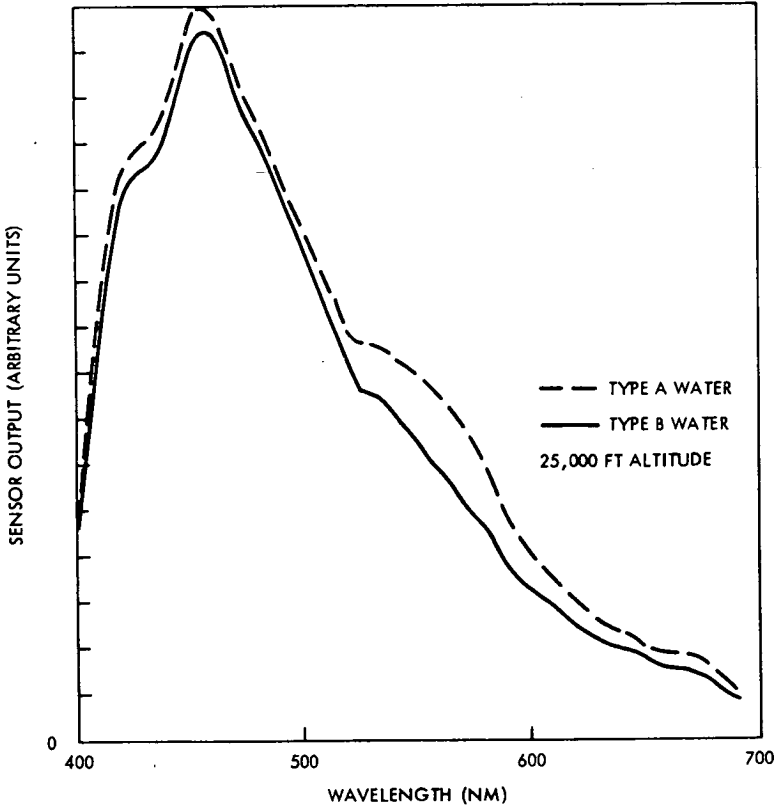


FIGURE 2. UNREDUCED SENSOR OUTPUT SIGNAL - 25,000 FT ALTITUDE

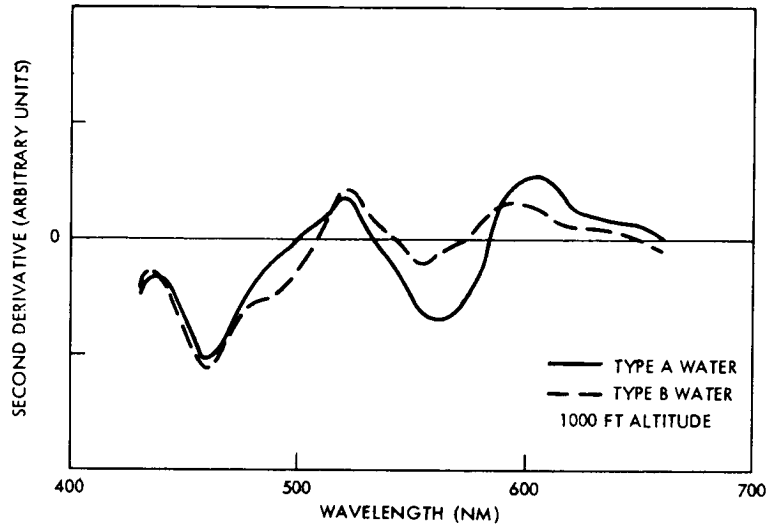


FIGURE 3. SECOND DERIVATIVES - 1000 FT ALTITUDE

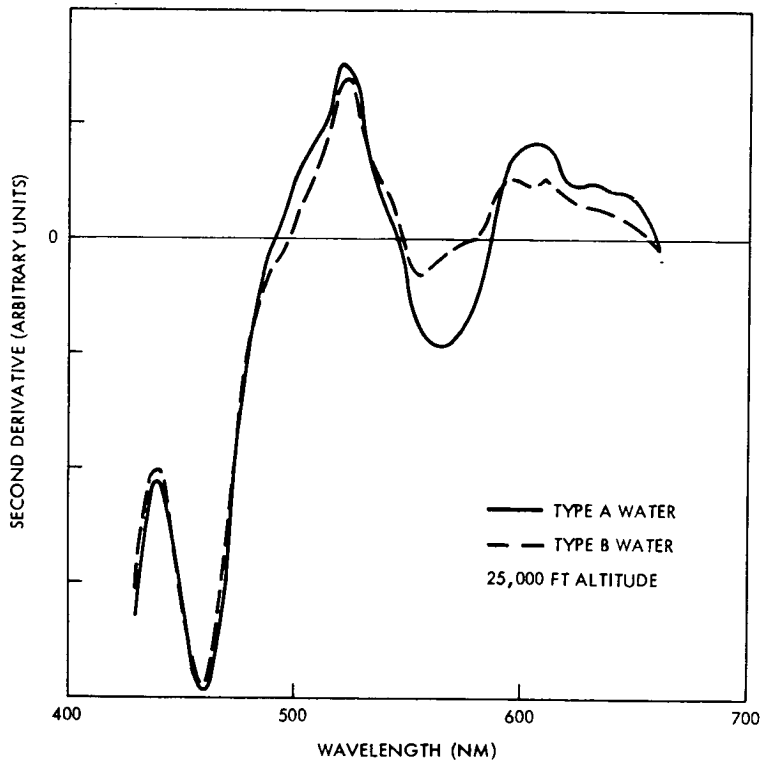


FIGURE 4. SECOND DERIVATIVES - 25,000 FT ALTITUDE

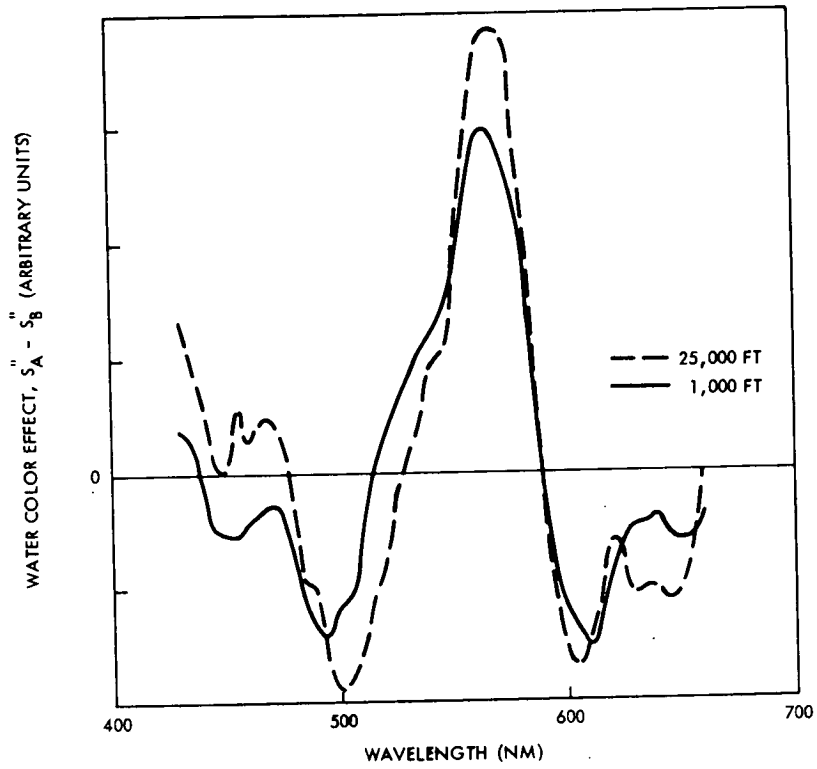


FIGURE 5. WATERCOLOR EFFECT ON SECOND DERIVATIVE

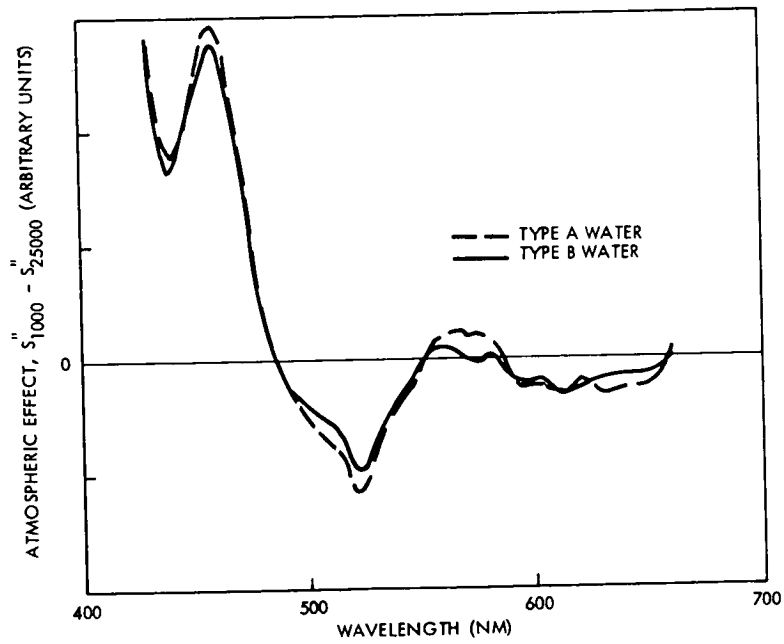


FIGURE 6. ATMOSPHERIC EFFECT ON SECOND DERIVATIVE

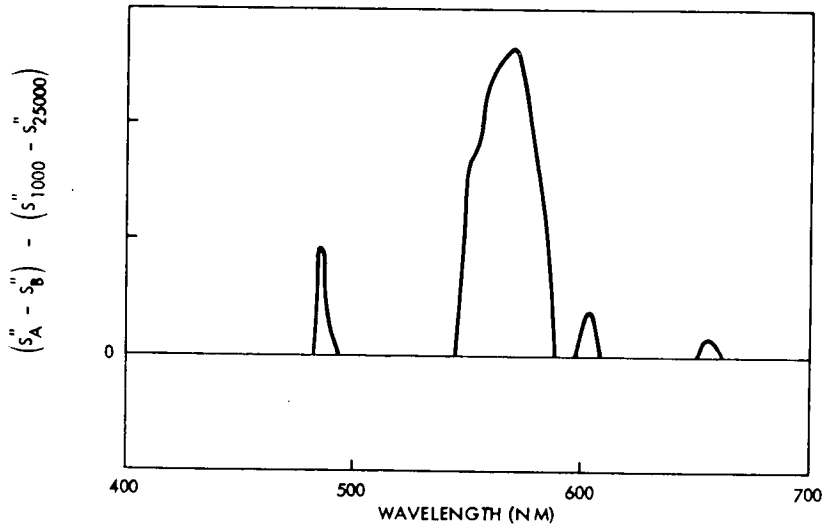


FIGURE 7. SPECTRAL REGIONS WHERE WATERCOLOR EFFECTS PREDOMINATE OVER ATMOSPHERIC EFFECTS

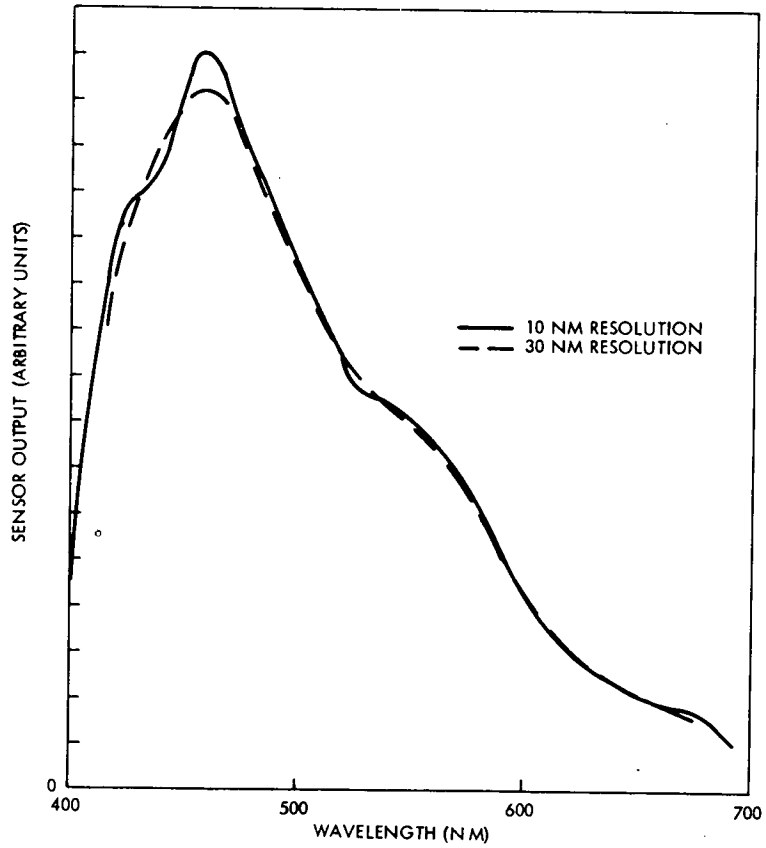


FIGURE 8. EFFECT OF SENSOR SPECTRAL RESOLUTION ON RAW DATA



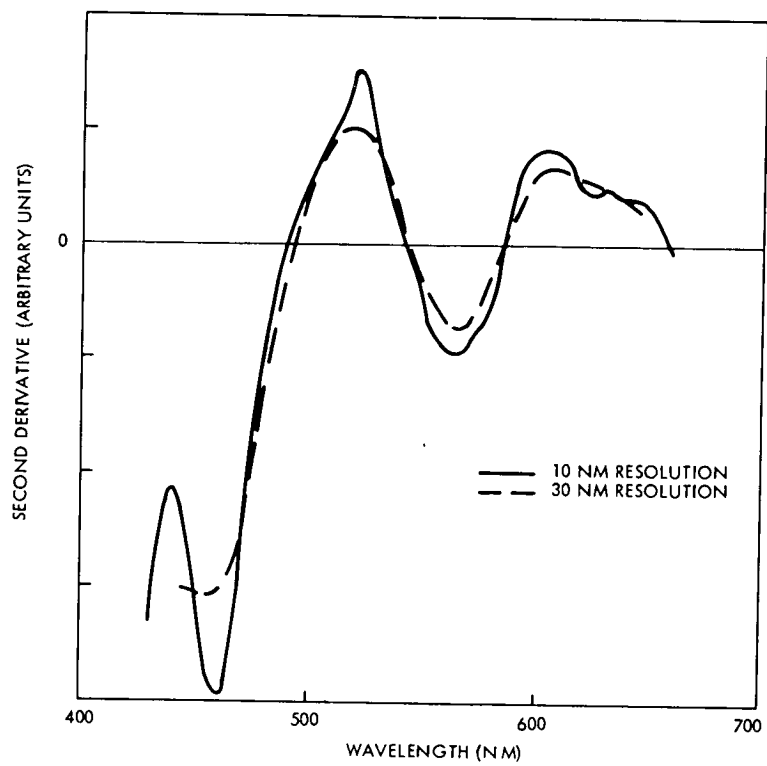


FIGURE 9. EFFECT OF SENSOR SPECTRAL RESOLUTION ON SECOND DERIVATIVE

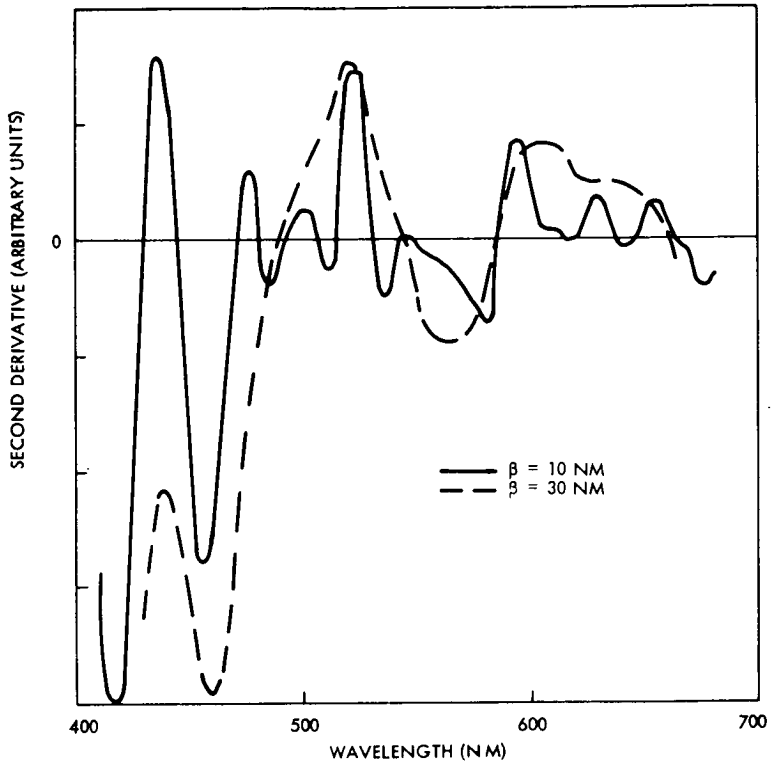


FIGURE 10. EFFECT OF FILTER PARAMETER  $\beta$  ON SECOND DERIVATIVE

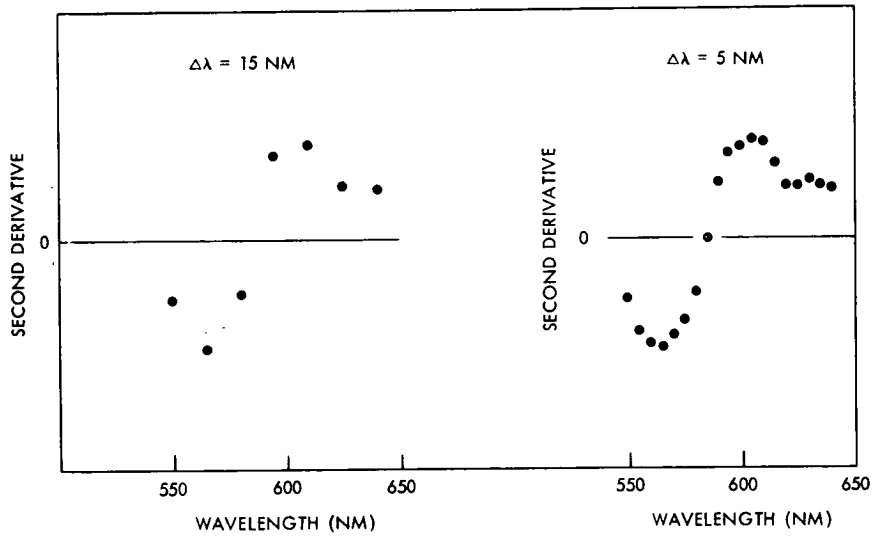


FIGURE 11. EFFECT OF SAMPLING RATE ON SECOND DERIVATIVE CURVE